MAGNETIC FIELDS IN STAR-FORMING CLOUDS: HOW CAN FIRST CONTRIBUTE?

B.C. Matthews[1], C.D. Wilson[1], and J.D. Fiege[2]

[1]Department of Physics & Astronomy, McMaster University, Hamilton, ON, Canada
[2]Canadian Institute for Theoretical Astrophysics, University of Toronto, Toronto, ON, Canada

Abstract

The SCUBA polarimeter at the James Clerk Maxwell Telescope has been used to probe the magnetic field geometry within the OMC-3 region of the Integral Filament of Orion A, the Barnard 1 cloud in Perseus and the B2 core in the ρ Ophiuchus dark cloud. In the submillimetre, polarized dust emission arises from rapidly spinning dust grains aligned by the local magnetic field. Although the polarized emission from each grain is orthogonal to the local field direction, a variation of the magnetic field orientation through the cloud can produce complex polarization patterns from which the field geometry cannot easily be determined without modelling. In each of the regions observed, the polarization patterns are inconsistent with strictly uniform or unidirectional magnetic fields on extended spatial scales. In each case, a decrease in polarization percentage is observed toward higher total intensities. In OMC-3, we have modelled the polarization pattern as arising from a bent filamentary cloud threaded by a helical magnetic field. The model is remarkably consistent with the polarization pattern observed.

Key words: ISM: clouds, magnetic fields, molecules — polarization — stars: formation — submillimetre

1. Introduction

The role of magnetic fields in the formation and evolution of molecular clouds and the star formation ongoing within them has long been a topic of debate. Over the last decade, polarized emission from rapidly spinning dust grains aligned by magnetic fields has been detected from the far-infrared to the millimeter regimes. Such detections establish the presence of fields, but cannot determine how important they are to star formation, since polarization does not yield field strength and detections have been limited to bright cores, making a sampling of large scale field geometry impossible. The installation of a polarimeter on the very sensitive Submillimetre Common User Bolometric Array (SCUBA) at the James Clerk Maxwell Telescope permits larger scale imaging polarimetry toward both cores and larger scale gas structures inside molecular clouds.

We have used the SCUBA polarimeter to detect polarized emission from dust in OMC-3 (part of the Orion A Integral Filament) and portions of the Barnard 1 (Perseus) and ρ Ophiuchus dark clouds.

2. The OMC-3 Region in Orion A

Figure 1 illustrates the polarization pattern observed toward the OMC-3 filament. OMC-3 is the northernmost part of the Integral Filament, first discovered by Bally et al. (1987). The OMC-1 core behind the Orion Nebula is the most well-studied part of the Integral Filament. OMC-3 is less massive, more filamentary and contains isolated protostellar sized cores.

As discussed in Matthews & Wilson (2000) and Matthews et al. (2001), the polarization vectors of Figure 1 exhibit strong alignment with the filament orientation from the northern boundary to the MMS7 core. South of this position, the vectors smoothly rotate away from the north-south orientation of the Integral Filament, with offsets between 70-90° from the filament.

In many star-forming cores previously observed, a decrease in the percentage polarization is observed toward regions of increasing total intensity (e.g. Dotson et al. 2000). This "depolarization" feature is also observed along the filament axis in OMC-3. Figure 2 illustrates that the depolarization is not limited to the bright embedded cores, but is observed even in the inter-core region between MMS6 and MMS7. Thus, the depolarization is a feature of the *filament itself* and not necessarily of the embedded cores.

The polarization pattern of Figure 1 north of MMS7 and the radial distribution of the polarization percentage of Figure 2 bear striking resemblance to the polarization patterns predicted by a recent model for filamentary molecular clouds threaded by helical magnetic fields (cf. Fig. 1 of Fiege & Pudritz 2000b). In the case of a toroidally-dominated helical field pattern, one expects to see polarization vectors align parallel to the filament axis and depolarization along the length of the axis, as observed in OMC-3.

2.1. A Model of OMC-3

The mis-alignment of the vectors from the filament in the south of OMC-3 must be addressed in order to properly

Proc. Symposium *'The Promise of the Herschel Space Observatory'* 12–15 December 2000, Toledo, Spain
ESA SP-460, July 2001, eds. G.L. Pilbratt, J. Cernicharo, A.M. Heras, T. Prusti, & R. Harris

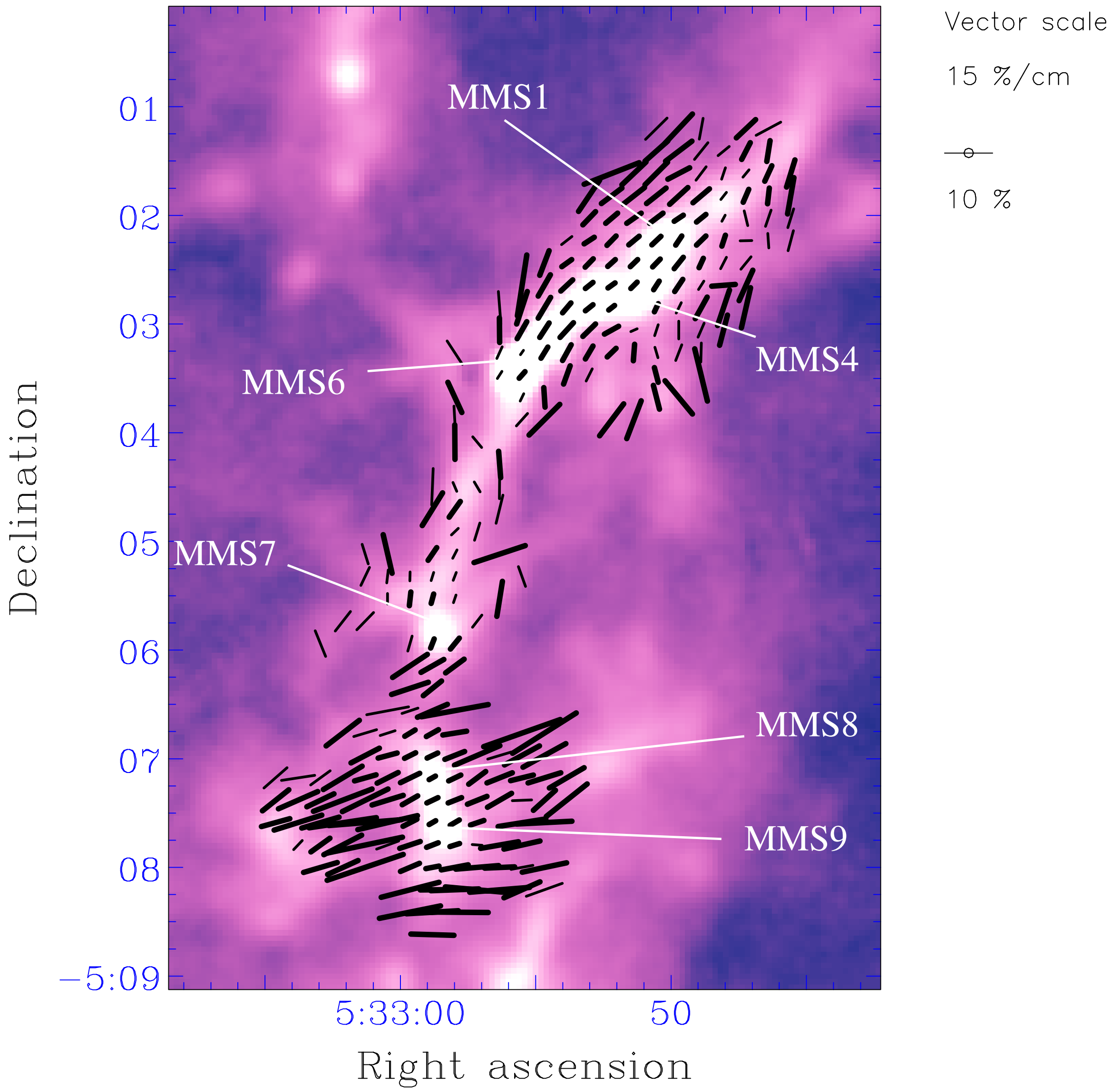

Figure 1. The 850 μm polarization pattern is overlaid on a larger SCUBA map (Johnstone & Bally 1999). Polarization vectors are binned to 12″, close to the 14″ beam size of the JCMT. The length of the vectors represents the polarization percentage, while the orientation indicates the net polarization direction detected. Increasing vector width reveals increasing S/N of the polarization measurement: thin vectors are at least 6σ while bold vectors are at least 10σ. Vectors with random uncertainty less than 1% are plotted, and bold vectors are accurate in position angle to better than 3°. The embedded cores are labelled MMS1 through MMS9 as designated by Chini et al. (1997). The coordinates are B1950.

model the entire polarization pattern. In the context of the helical field model, such a pattern could be produced by: poloidal dominance of the field structure; a bend in the filament south of MMS7; or a second, fainter filament oriented orthogonal to the Integral Filament.

Figure 3 presents a qualitative model of OMC-3 where the filament is bent into an arc in its southern half and then rotated in the plane of the sky until a similar pattern to OMC-3 is produced. The asymmetry is produced when the filament is bent because toroidal components of the field are compressed on the inner part of the bend and expanded on the other. Where compression occurs, the magnetic field becomes stronger and dominates the polarization pattern. Matthews et al. (2001) discuss this model in more detail and present a qualitative model of crossed filaments as well.

3. The Dark Clouds

Figure 4 shows the polarization pattern from the B2 core of the ρ Ophiuchus dark cloud ($d = 160$ pc). Vectors exhibit varying orientation over the core and appear to align

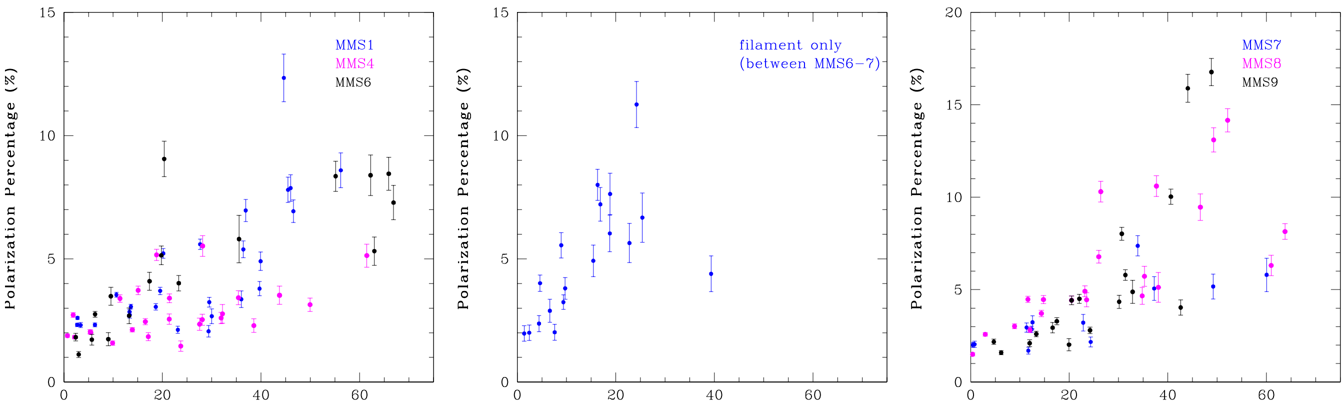

Figure 2. These plots show the variation in polarization percentage with distance from the filament axis for different regions of OMC-3. The decrease in polarization percentage toward the axis is evident in Figure 1. The distance plotted along the x-axis refers to a displacement orthogonal to the local filament orientation. The left and right panel show data for regions containing bright cores as labelled. The central panel shows the region between MMS6 and MMS7; although no cores are present, depolarization is still observed. Thus, filamentary models must address depolarization as a key component of their field structure.

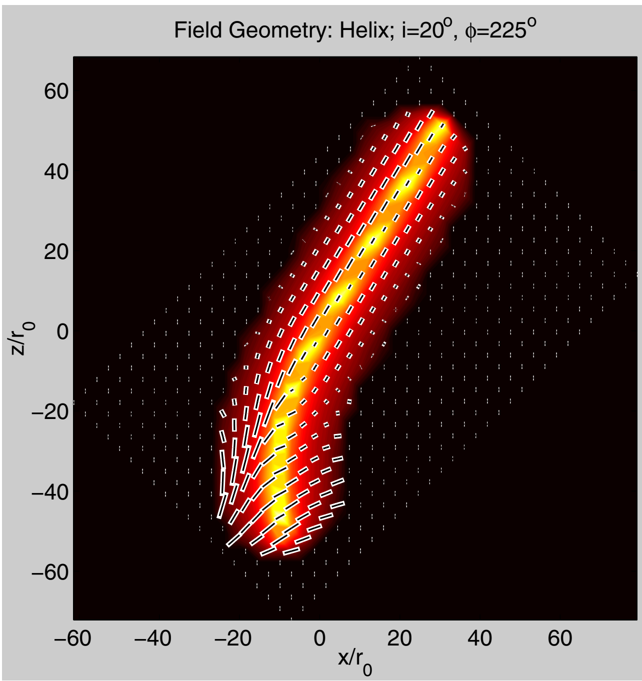

Figure 3. A model of OMC-3 based on a helical field wrapping the filament (Fiege & Pudritz 2000a). This is not a fit to the data of Figure 1, merely an example of a possible geometry which can be produced by a filament bent in the south with a helical field running along its length. The filament is inclined by 20° to the plane of the sky and has been rotated 225° about its axis.

haps because we have not probed the material far enough from the B2 peak.

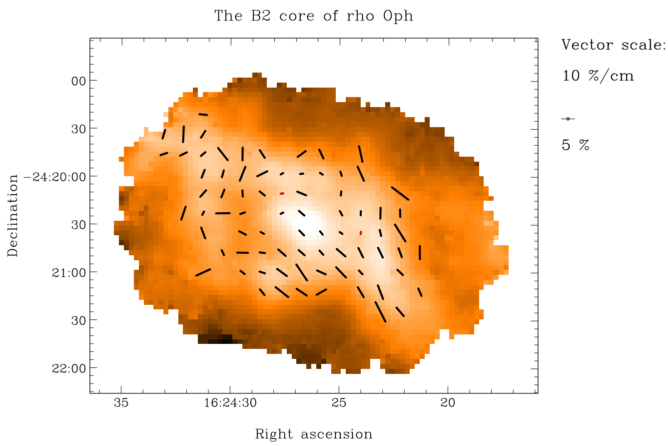

Figure 4. The B2 core of ρ Ophiuchus represents the smallest spatial scale map in our sample. The polarization pattern appears less ordered than those of OMC-3 and Barnard 1. However, significant polarization is still detected. All data are binned to 12″ are uncertain to < 1%. All vectors have S/N better than 3σ (in polarization percentage), which indicates a maximum uncertainty of 9° in position angle. Red vectors have a polarization percentage value of 1% or less and should be interpreted with caution. There is some alignment observed between the polarization data and the faint underlying gas structure surrounding the peak. Coordinates are B1950.

with the faint dust emission at the edges. As in OMC-3, these data are suggestive of a correlation between magnetic field geometry and gas structure. B2 exhibits some depolarization toward the bright central core, but it is not as pronounced as that of Barnard 1 (shown below) per-

Figure 5 shows the polarization pattern observed toward part of the dark cloud Barnard 1 in Perseus (d = 350 pc). The polarization pattern off the cores is remarkably uniform with vectors aligned primarily in an east to west orientation. Within each core, the orientations are also uniform but mis-aligned from the surrounding cloud.

Within the northern source, the vectors lie at a position angle of $\sim 50°$ E of N, while the southeast binary source ranges smoothly from $-50°$ to $65°$ E of N. The faintest source to the west aligns well with the ambient cloud, at $90°$ E of N. Taken as a whole, the Barnard 1 polarization pattern does not support the idea that a uniform magnetic field threads the cloud and its embedded cores.

The cores show depolarization compared to the percentage polarizations measured in the ambient cloud, which reach 10%. Within the cores, the values are typically less than 5%. Whether this effect is due to tangled field lines on small scales (as observed in the much larger OMC-1 core with BIMA; Rao et al. 1998), grain physics or field geometry is not yet known.

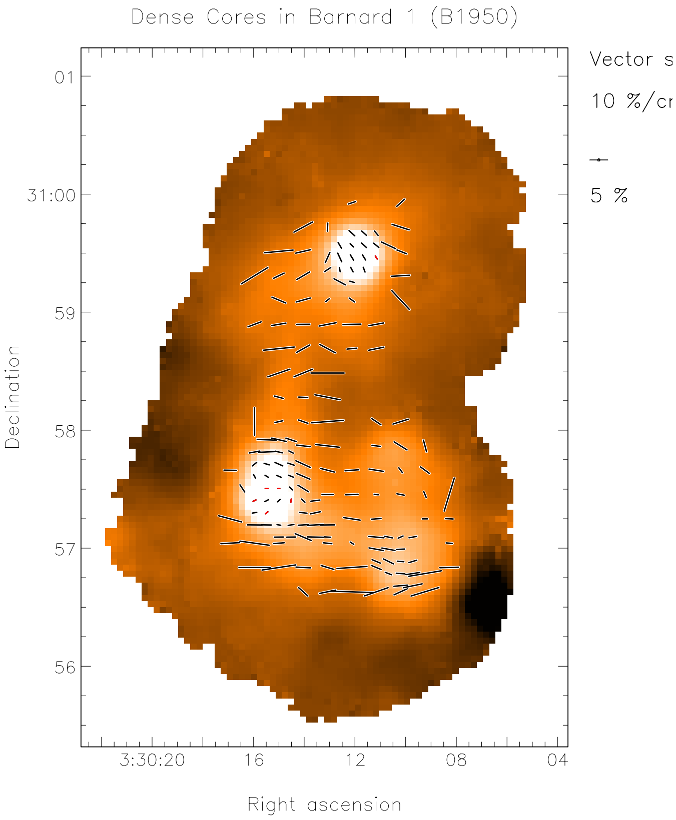

Figure 5. This portion of the Barnard 1 cloud exhibits polarized emission aligned roughly east-west with higher polarization percentages off the bright cores. The data are binned to 12″ in low intensity regions, and 6″ in high intensity regions where the signal-to-noise ratio is higher. The constrains on vectors plotted are identical to those for Figure 4.

4. Discussion

Models of emission from aligned, spinning dust grains reveal that the net polarization direction emitted from each grain is perpendicular to the plane of sky magnetic field component. For this reason, magnetic field geometry is typically interpreted as orthogonal to the polarization pattern observed longward of 100 μm (Hildebrand 1988). Within cores, polarization patterns are usually smoothly varying, so magnetic fields were interpreted as uniform or smoothly varying as well. Across larger scales in our SCUBA maps, significant variations in polarization vector orientation exist. The changes in orientation may be abrupt, making interpretations of field geometry more complex. If the field geometry varies through the depth of a cloud, then simply rotating the polarization vectors could produce a mis-leading interpretation of the magnetic field's true geometry.

In our data, evidence for correlation between field geometry and heightened column density exists, since polarization vectors are observed to follow filamentary structures in OMC-3 and ρ Ophiuchus. The OMC-3 polarization pattern is well reproduced by a bent filament threaded by a toroidally-dominated helical field.

5. How Can FIRST Contribute?

The FIRST satellite will observe SO and CCS line emission on large scales toward molecular clouds. The lower frequency transitions of these lines are observable with the VLA (and in the future the SKA), but the FOV of these telescopes will be too small to survey widely for these molecules. CCS in particular produces significant Zeeman splitting in the presence of magnetic fields and is an excellent candidate for future line-of-sight magnetic field measurements at intermediate ($10^4 - 10^5$ cm^{-3}) densities inside molecular clouds. OH has traditionally been used, but despite dozens of observations, Zeeman splitting of OH has only been clearly detected toward 15 star-forming regions (Crutcher 1999). Other molecular line probes of magnetic field strengths are required to determine how significant a role is played by these fields in the evolution of molecular clouds and star formation.

FIRST's large FOV will provide large spatial scale maps of star-forming regions. Thus, it will identify more filamentary clouds and high density cores which can be followed up with polarimetry work with the JCMT, CSO, BIMA, OVRO, the SMA and eventually ALMA.

References

Bally, J., Langer, W., Stark, A., Wilson, R. 1987, ApJ 313, L45

Chini, R. Reipurth, B., Ward-Thompson, D., et al. 1997, ApJ 474, 135

Crutcher, R. 1999, ApJ 520, 706

Dotson, J., Davidson, J., Dowell, C.D., et al. 2000, ApJSS 128, 335

Fiege, J., Pudritz, R. 2000a, MNRAS 311, 85

Fiege, J., Pudritz, R. 2000b, ApJ 544, 830

Hildebrand, R. 1988, QJRAS 29, 327

Johnstone, D. Bally, J. 1999, ApJ 510, L49

Matthews, B. Wilson, C. 2000, ApJ, 531, 868

Matthews, B. Wilson, C. Fiege, J. 2001, in preparation

Rao, R., Crutcher, R., Plambeck, R., Wright, M. 1998, ApJ 502, 75